ELSEVIER

Journal of Quantitative Spectroscopy & Radiative Transfer 105 (2007) 525–532

Journal of Quantitative Spectroscopy & Radiative Transfer

www.elsevier.com/locate/jqsrt

Note

Speed-dependent Voigt profile for water vapor in infrared remote sensing applications

Chris D. Boone[a,*], Kaley A. Walker[b], Peter F. Bernath[a,c]

[a]*Department of Chemistry, University of Waterloo, Waterloo, Ont., Canada N2L 3G1*
[b]*Department of Physics, University of Toronto, Toronto, Ont., Canada M5S 1A7*
[c]*Department of Chemistry, University of York, Heslington, York YO10 5DD, UK*

Received 8 August 2006; received in revised form 17 November 2006; accepted 23 November 2006

Abstract

The Voigt profile does not provide a sufficiently accurate representation of the line shape for air-broadened H_2O vapor over a significant range of conditions commonly encountered in atmospheric remote sensing. A speed-dependent Voigt profile yields much improved residuals in the analysis of water from infrared measurements collected by the atmospheric chemistry experiment (ACE), a satellite mission for remote sensing of the Earth's atmosphere. An analytical expression is presented for the rapid calculation of the speed-dependent Voigt profile.

Keywords: Water; Line shape; Speed-dependent Voigt; Remote sensing

1. Introduction

SCISAT-1, otherwise known as the atmospheric chemistry experiment (ACE), is a Canadian-led satellite mission for remote sensing of the Earth's atmosphere, launched August 2003 into a circular orbit inclined 74° to the equator [1]. The primary instrument is the ACE-FTS, a Fourier transform spectrometer featuring high resolution ($0.02\,cm^{-1}$, corresponding to a ± 25 cm maximum optical path difference) and broad spectral coverage in the infrared ($750–4400\,cm^{-1}$). The ACE-FTS works primarily in the solar occultation mode, collecting atmospheric limb measurements using the sun as a radiation source.

Analysis of ACE-FTS measurements revealed a line shape problem endemic to water. For altitudes below which the pressured-broadened line width exceeded the instrumental line width (and the actual line shape was therefore observable), significant w-shaped residuals occurred for H_2O but were not observed for any other molecule. It was not possible to reproduce the observed H_2O line shapes through adjusting the typical set of spectroscopic line parameters found in linelists such as the HITRAN 2004 database [2].

The problem resides not in the spectroscopic parameters, but rather in the underlying assumptions associated with the calculation. The Voigt profile, a convolution of Doppler and Lorentzian line shape

*Corresponding author. Tel.: 1 519 888 4814; fax: 1 519 746 0435.
E-mail address: cboone@uwaterloo.ca (C.D. Boone).

0022-4073/$ - see front matter © 2006 Elsevier Ltd. All rights reserved.
doi:10.1016/j.jqsrt.2006.11.015

functions, is the standard approach for calculating the line shape for infrared atmospheric remote sensing. However, the Voigt profile calculation assumes that the pressure and Doppler broadening are uncorrelated and that changes of velocity during collisions can be neglected. Based on observations from the ACE-FTS measurements, at least one of these assumptions clearly breaks down for air-broadened H_2O vapor over a significant range of pressures typically encountered in atmospheric remote sensing.

Various alternatives exist to the Voigt line shape [3]. It has been shown that the Galatry line shape [4], derived from an approach that uses a soft-collision model for velocity-changing collisions, does not appear to be appropriate for remote sensing applications because the associated parameters vary nonlinearly with pressure [3,5], suggesting that the neglected correlation between molecular relaxation and the Doppler effect plays a significant role [6]. For the analysis of H_2O in ACE-FTS measurements, we choose the speed-dependent Voigt profile. A rapid analytical approach is presented for the calculation of this line shape, convenient for atmospheric applications because it also allows one to calculate analytical derivatives with respect to the spectroscopic parameters.

2. Speed-dependent Voigt profile

The speed-dependent Voigt (SDV) profile is the real part of the Fourier transform of the polarization correlation function $\Phi(t)$:

$$I(\omega) = \frac{1}{\pi}\,\mathrm{Re}\left[\int_0^\infty \mathrm{e}^{-\mathrm{i}\omega t}\Phi(t)\,\mathrm{d}t\right]. \tag{1}$$

For the SDV profile, the polarization correlation function is [7]

$$\Phi(t) = \frac{\exp[\mathrm{i}\omega_\mathrm{o}t - (\Gamma_\mathrm{o} - \frac{3}{2}\Gamma_2)t]}{(1+\Gamma_2 t)^{3/2}}\exp\left[-\left(\frac{\omega_\mathrm{o}v_\mathrm{a}t}{2c}\right)^2\frac{1}{1+\Gamma_2 t}\right], \tag{2}$$

where ω_o is the line center frequency, c is the speed of light, Γ_o is the mean relaxation rate over absorber speeds, Γ_2 is a phenomenological relaxation rate that accounts for the speed dependence of the relaxation, and v_a is the most probable speed of the absorbing molecule:

$$v_\mathrm{a} = \sqrt{\frac{2k_\mathrm{B}T}{m}}, \tag{3}$$

where k_B is the Boltzmann constant, T is temperature in Kelvin, and m is molecule's mass.

The Fourier transform of Eq. (2) can be written as

$$I(\omega) = \frac{2}{\pi\Gamma_2}\mathrm{Re}\left[\mathrm{e}^{x+2y}\int_0^1 \exp\left[-\left(yz^2 + \frac{x+y}{z^2}\right)\right]\mathrm{d}z\right],$$

where

$$z = (1+\Gamma_2 t)^{-1/2}, \quad x = \left(\frac{\Gamma_\mathrm{o}}{\Gamma_2} - \frac{3}{2}\right) + \mathrm{i}\frac{(\omega-\omega_\mathrm{o})}{\Gamma_2} \equiv \alpha + \mathrm{i}\beta,$$

$$y = \frac{1}{\Gamma_2^2}\frac{\omega_\mathrm{o}^2 k_\mathrm{B}T}{2mc^2} \tag{4}$$

which evaluates to the following expression:

$$I(\omega) = \frac{1}{2\sqrt{\pi}}\sqrt{\frac{2mc^2}{\omega_\mathrm{o}^2 k_\mathrm{B}T}}\,\mathrm{Re}[\exp[z_1^2]\mathrm{erfc}(z_1) - \exp[z_2^2]\mathrm{erfc}(z_2)], \tag{5}$$

where

$$z_1 = \frac{1}{\sqrt{2}}\left[\sqrt{\sqrt{(y+\alpha)^2+\beta^2}+y+\alpha} + \mathrm{i}\,\mathrm{sign}(\beta)\sqrt{\sqrt{(y+\alpha)^2+\beta^2}-y-\alpha}\right] - \sqrt{y},$$
$$z_2 = z_1 + 2\sqrt{y}. \tag{6}$$

The function erfc( ) is the complementary error function, and the function sign(β) is $+1$ if β is positive, 0 if β is zero, and -1 if β is negative.

The expression in Eq. (5) involves the difference of two terms, each of which can be evaluated using the implementation of the Humlicek algorithm described in the paper by Kuntz [8] (with the appropriate corrections [9]), where accurate analytical approximations are given for functions of the following form:

$$K(a,b) = \mathrm{Re}(\exp(z^2)\mathrm{erfc}(z)), \quad z = a - \mathrm{i}b. \tag{7}$$

To account for the complex nature of the relaxation rate, the following substitutions are made [10]:

$$\Gamma_\mathrm{o} = \gamma_\mathrm{o} - \mathrm{i}\eta_\mathrm{o}, \quad \Gamma_2 = \gamma_2 - \mathrm{i}\eta_2. \tag{8}$$

With these substitutions, the calculation of the SDV profile becomes more complicated. The expressions for the parameters z_1 and z_2 from Eq. (5) become

$$z_1 = \frac{1}{\sqrt{2}}\left[\sqrt{\sqrt{p^2+q^2}+p} - \sqrt{\sqrt{r^2+s^2}+r}\right] + \frac{1}{\sqrt{2}}\mathrm{i}\left[\mathrm{sign}(q)\sqrt{\sqrt{p^2+q^2}-p} - \mathrm{sign}(s)\sqrt{\sqrt{r^2+s^2}-r}\right],$$
$$z_2 = \frac{1}{\sqrt{2}}\left[\sqrt{\sqrt{p^2+q^2}+p} + \sqrt{\sqrt{r^2+s^2}+r}\right] + \frac{1}{\sqrt{2}}\mathrm{i}\left[\mathrm{sign}(q)\sqrt{\sqrt{p^2+q^2}-p} + \mathrm{sign}(s)\sqrt{\sqrt{r^2+s^2}-r}\right], \tag{9}$$

where

$$p = \frac{\gamma_\mathrm{o}\gamma_2}{\gamma_2^2+\eta_2^2} - \frac{3}{2} - \frac{(\omega-\omega_\mathrm{o})\eta_2}{\gamma_2^2+\eta_2^2} + \frac{\omega_\mathrm{o}^2 k_\mathrm{B} T}{2mc^2}\frac{\gamma_2^2-\eta_2^2}{(\gamma_2^2+\eta_2^2)^2} + \frac{\eta_\mathrm{o}\eta_2}{\gamma_2^2+\eta_2^2},$$
$$q = \frac{\gamma_\mathrm{o}\eta_2 - \gamma_2\eta_\mathrm{o}}{\gamma_2^2+\eta_2^2} + \frac{(\omega-\omega_\mathrm{o})\gamma_2}{\gamma_2^2+\eta_2^2} + \frac{\omega_\mathrm{o}^2 k_\mathrm{B} T}{2mc^2}\frac{2\gamma_2\eta_2}{(\gamma_2^2+\eta_2^2)^2},$$
$$r = \frac{\omega_\mathrm{o}^2 k_\mathrm{B} T}{2mc^2}\frac{\gamma_2^2-\eta_2^2}{(\gamma_2^2+\eta_2^2)^2},$$
$$s = \frac{\omega_\mathrm{o}^2 k_\mathrm{B} T}{2mc^2}\frac{2\gamma_2\eta_2}{(\gamma_2^2+\eta_2^2)^2}. \tag{10}$$

If the η_2 term is negligible, it is preferable to use the much simpler expressions in Eq. (6), with the following substitution:

$$(\omega-\omega_\mathrm{o}) \to (\omega-\omega_\mathrm{o}-\eta_\mathrm{o}), \tag{11}$$

where η_o is obviously the well-known pressure shift, traditionally assumed to be proportional to pressure. The broadening and narrowing parameters, γ_o and γ_2, are proportional to pressure (P) and are assumed to have a power law dependence with respect to temperature (T) [2]:

$$\gamma(P,T) = \gamma(T_\mathrm{o})P\left(\frac{T_\mathrm{o}}{T}\right)^n, \tag{12}$$

where the reference temperature, T_o, is 296 K. The parameter $\eta_2(P,T)$ is also assumed here to follow the pressure and temperature dependence described in Eq. (12), and all parameters (γ_o, γ_2, and η_2) are assumed to have a common value for temperature dependence exponent (n).

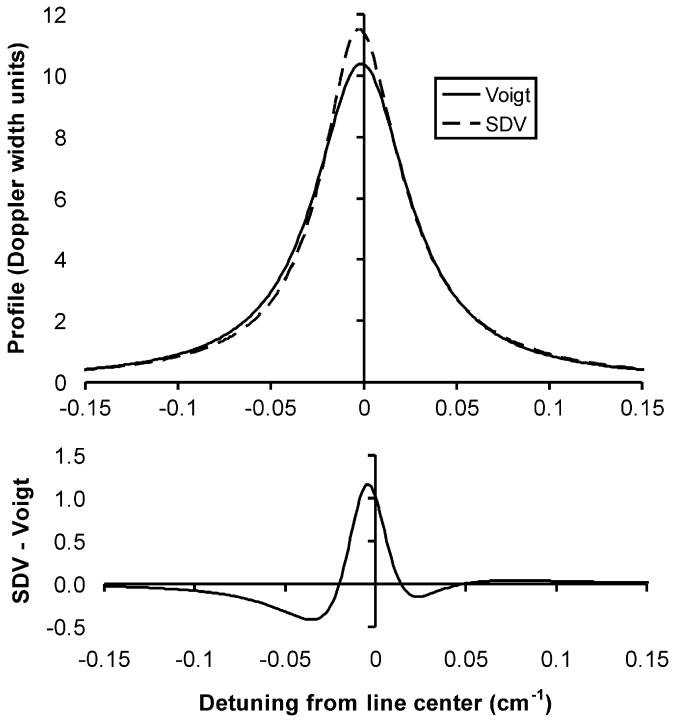

Fig. 1. Comparison of Voigt and speed-dependent Voigt profiles. The parameters used in the calculations are described in the text.

The formulation presented here fails if the parameter γ_2 is fixed to zero (division by zero). However, setting the parameter to a very small value yields minimal deviation from a Voigt profile.

Fig. 1 shows the difference between the Voigt and SDV profiles for a common broadening parameter. The SDV profile is calculated from the expression in Eq. (5) using the parameters z_1 and z_2 defined in Eqs. (9) and (10). The Voigt profile uses an air-broadening half-width (the equivalent of $\gamma_o(T_o)$) of $0.095\,cm^{-1}\,atm^{-1}$. The SDV profile uses the following parameters: $\gamma_o(T_o) = 0.095\,cm^{-1}\,atm^{-1}$, $\gamma_2(T_o) = 0.03\,cm^{-1}\,atm^{-1}$, and $\eta_2(T_o) = 0.015\,cm^{-1}\,atm^{-1}$. The temperature dependence exponent (n in Eq. (12)) is set to 0.77 for both Voigt and SDV profiles, and the pressure shift parameter, η_o/P, is set to $0.005\,cm^{-1}\,atm^{-1}$ for both profiles. Temperature in the calculations is 215 K, and pressure is 0.25 atm.

The SDV profile is narrower than the Voigt profile, giving rise to the w-shaped structure in the difference between the two profiles. The asymmetry in the SDV profile in Fig. 1 is a consequence of the η_2 term, but it is worth noting that the pressure shift term (η_o) can lead to an apparent asymmetry for atmospheric limb measurements of molecular lines. Measuring through a medium with variable pressure, contributions to the signal from different pressures will have different line centers, leading to an apparent asymmetry. The η_2 term, conversely, induces an actual asymmetry in the line even under static pressure conditions.

3. H_2O retrievals from ACE-FTS measurements

The approach used for ACE-FTS volume mixing ratio (VMR) retrievals is described elsewhere [11]. Briefly, pressure and temperature as a function of altitude are determined through analysis of CO_2 lines in the spectra, making use of an assumed VMR profile for CO_2. Pressure and temperature are then fixed in the subsequent VMR retrievals for other molecules (and for the analysis presented here).

The ACE-FTS retrieval software was updated to allow the determination of line shape parameters simultaneously with the VMR retrieval. To test the effectiveness of the SDV line shape, retrievals were performed on a $0.63\,cm^{-1}$ wide window centered at $2672.71\,cm^{-1}$ over an altitude range 7–21 km. This window contains a single HDO line at $2672.59\,cm^{-1}$. Fig. 2 shows the data being analyzed, the target HDO line for a series of 15 ACE-FTS measurements over the course of a single occultation (sr10909, collected

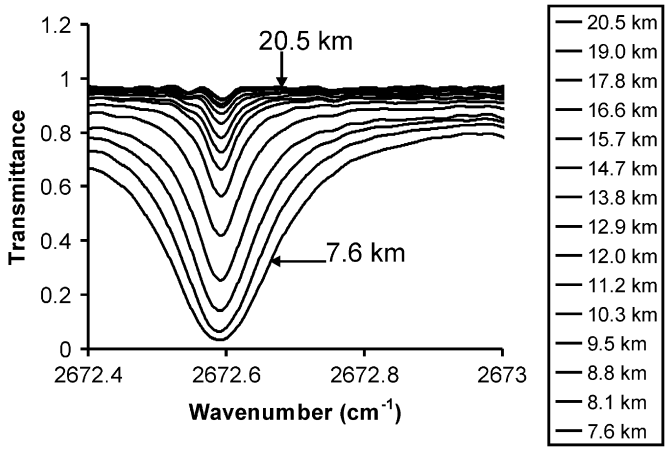

Fig. 2. An HDO line at 2672.59 cm^{-1} for a series of 15 measurements in sr10909, an occultation collected August 22, 2005 at latitude 10°S and longitude 7°W.

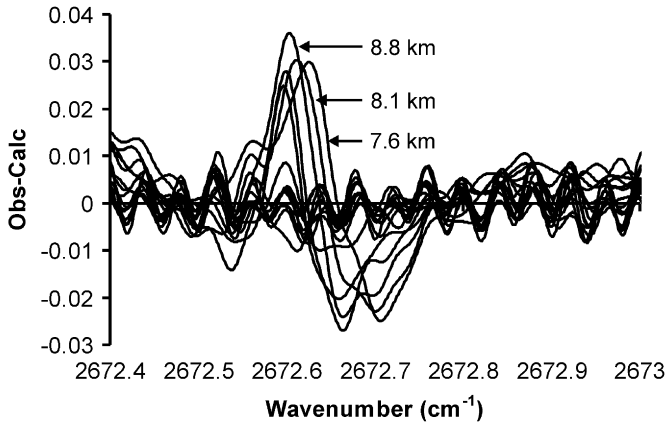

Fig. 3. For the measurement set depicted in Fig. 2, fitting residuals when using a Voigt line shape and spectroscopic parameters from the HITRAN 2004 line list. The residuals for all 15 measurements are plotted simultaneously.

August 22, 2005 at latitude 10°S and longitude 7°W). The heights listed to the right of the figure are the measurement tangent altitudes (altitudes of closest approach to the Earth for solar rays being measured). As one probes lower and lower into the atmosphere, the absorption depth increases (due to more HDO molecules along the line of sight), and the line broadens (due to pressure broadening).

Fig. 3 shows the residuals obtained when fitting for HDO VMR using the standard Voigt profile, and using the spectroscopic parameters from the HITRAN 2004 line list. Curves for all 15 analyzed measurements are plotted on a common graph. The residuals for the lowest altitude measurements are very large, clear evidence of line shape problems. There is also significant asymmetry in the line (one lobe dips lower than the other). The asymmetry does not vary much with altitude, suggesting that there is a true asymmetry in the line, not just an apparent asymmetry resulting from the pressure shift effects mentioned previously.

Note the presence of a fixed pattern in the residuals from different measurements, a consequence of far wing contributions from lines not included in the calculation, and perhaps a degree of residual channeling in the transmittances. The effective signal-to-noise ratio in this window, defined by the amplitude of this oscillatory fixed pattern, is roughly 300 to 1.

It is possible to improve the residuals by adjusting the pressure-broadening parameter. Fig. 4 shows the residuals when the pressure-broadening half-width is treated as a fitting parameter rather than fixed to the value from the HITRAN 2004 line list. Note that the temperature dependence exponent is fixed to the value

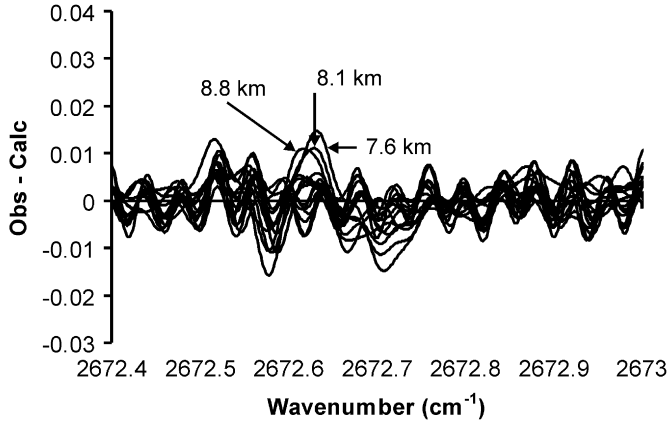

Fig. 4. The same as Fig. 3, but with the air-broadened half-width fitted rather than fixed to the value from the HITRAN 2004 line list.

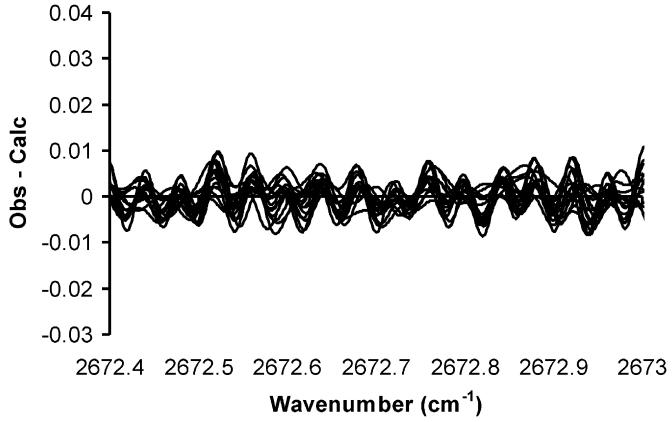

Fig. 5. The same as Fig. 3, but using a speed-dependent Voigt line shape rather than a Voigt line shape. The parameters required for the speed-dependent Voigt profile (not available in any line list) were determined via least-squares fitting.

from the line list. There is a significant improvement in the fitting results, but there remain features in the residuals for the lowest altitude measurements.

Fig. 5 shows the residuals for analyzing the HDO line using an SDV profile. The fitting parameters (in addition to HDO VMR) were $\gamma_o(T_o)$, $\gamma_2(T_o)$, $\eta_2(T_o)$, and a pressure shift parameter, η_o/P. Again, the temperature dependence exponent, n, is fixed to the value in the HITRAN 2004 linelist and is assumed to be the same for γ_o, γ_2, and η_2. The residuals in Fig. 5 are below the level of the effective noise.

4. Discussion

The Voigt profile is not sufficiently accurate to calculate air-broadened infrared H_2O lines measured by the ACE-FTS instrument. The low mass of H_2O compared to its collision partners (N_2 and O_2) is a major contribution to the breakdown of the assumptions implicit in the calculation of the Voigt profile. However, the significant dipole moment of water likely also plays a role, through increasing the influence range of collisions, because the effect is not observed for CH_4.

Self-broadening of water lines is ignored in the analysis of ACE-FTS spectra. The lowest altitudes studied with the ACE-FTS are near 5 km, and the partial pressure of water at these altitudes (and above) is never large enough for self-broadening effects to become significant. For the analysis of the HDO line presented in this article, for example, the VMR at the lowest analyzed measurement was less than 0.0002 ppv. The self-broadening parameters for water will be subject to speed-dependent effects, similar to the air-broadening

parameters described here. Speed-dependent effects generally decrease with the mass of the collision partner, so one might expect less of an effect for self-broadening compared to air broadening. However, stronger interactions via the dipole moment of water may serve to enhance the effects despite the reduced collision partner mass.

Using a speed-dependent Voigt profile for water clearly represents a dramatic improvement in the calculation accuracy, and adopting this line shape should therefore improve the accuracy of the H_2O retrievals from ACE-FTS. The primary stumbling block in using a speed-dependent Voigt profile for water is the current lack of information on the $\gamma_o(T_o)$, $\gamma_2(T_o)$, and $\eta_2(T_o)$ parameters. Note that the interpretation of $\gamma_o(T_o)$ is in theory equivalent to the broadening parameter currently in linelists such as HITRAN 2004, but the values of $\gamma_o(T_o)$ obtained using a speed-dependent Voigt profile will generally be slightly larger [5]. It is therefore not appropriate to leave the broadening parameter in the linelist fixed and add new columns for $\gamma_2(T_o)$ and $\eta_2(T_o)$. All of the parameters need to be determined simultaneously from experimental data.

In the absence of the necessary linelist data for $\gamma_o(T_o)$, $\gamma_2(T_o)$, and $\eta_2(T_o)$, an interim set of these parameters will be generated from the ACE-FTS spectra for all water lines used in retrievals at low altitudes (below $\sim$15 km), including lines used in the retrieval of H_2O VMR profiles and lines that serve as interferences in the retrieval of other molecules. This should in particular improve the results for weak absorbers such as, e.g., HFC-134a and peroxyacetyl nitrate (PAN), molecules for which the huge residuals from overlapping water lines have created challenges in the retrieval process. Several dozen occultations will be analyzed simultaneously in order to improve the accuracy of the derived parameters.

In principle, the effects requiring the use of a speed-dependent Voigt profile extend to altitudes above 15 km, but the resolution of our instrument likely precludes us from generating accurate parameters in that altitude region. There is a great need for analysis of laboratory spectra of H_2O to generate the parameters required for the speed-dependent Voigt profile.

It should be stressed that the approach described here neglects the contribution of velocity and phase changing collisions to the line shape. The ACE-FTS measurements lack the sensitivity to determine how significant such contributions may be. If laboratory measurements indicate the need, the approach described here could be incorporated into the speed-dependent Nelkin–Ghatak profile [12], an empirical approach with a very simple form, albeit with the complication of requiring calculation of the imaginary component of the expression in Eq. (5).

Acknowledgments

Funding was provided by the Canadian Space Agency and the Natural Sciences and Engineering Research Council (NSERC) of Canada.

References

[1] Bernath PF, McElroy CT, Abrams MC, Boone CD, Butler M, Camy-Peyret C, et al. Atmospheric chemistry experiment (ACE): mission overview. Geophys Res Lett 2005;32:L15S01.
[2] Rothman LS, Jacquemart D, Barbe A, Benner DC, Birk M, Brown LR, et al. The HITRAN 2004 molecular spectroscopic database. JQSRT 2005;96:139–204.
[3] Lisak D, Hodges JT, Ciurylo R. Comparison of semiclassical line-shape models to rovibrational H_2O spectra measured by frequency-stabilized cavity ring-down spectroscopy. Phys Rev A 2006;73:012507.
[4] Galatry L. Simultaneous effect of Doppler and foreign gas broadening on spectral lines. Phys Rev 1961;122:1218–23.
[5] D'Eu J-F, Lemoine B, Rohart F. Infrared HCN lineshapes as a test of Galatry and speed-dependent Voigt profiles. J Mol Spectrosc 2002;212:96–110.
[6] Bielski A, Brym S, Ciurylo R, Szudy J. Experimental study of speed-dependent collisional effects of He and Ne on the 687.1 nm argon line. Eur Phys JD 2000;8:177–87.
[7] Rohart F, Colmont J-M, Wlodarczak G, Bouanich J-P. N_2- and O_2-broadening coefficients and profiles for millimeter lines of $^{14}N_2O$. J Mol Spectrosc 2003;222:159–71.
[8] Kuntz M. A new implementation of the Humlicek algorithm for the calculation of the Voigt profile function. JQSRT 1997;57:819–24.
[9] Ruyten W. Comment on "a new implementation of the Humlicek algorithm for the calculation of the Voigt profile function" by M. Kuntz [JQSRT 1997; 57(6): 819–824]. JQSRT 2004;86:231–3.

[10] Rohart F, Ellendt A, Kaghat F, Mader H. Self and polar foreign gas line broadening and frequency shifting of CH_3F: effect of speed dependence observed by millimeter-wave coherent transients. J Mol Spectrosc 1997;185:222–33.
[11] Boone CD, Nassar R, Walker KA, Rochon Y, McLeod SD, Rinsland CP, et al. Retrievals for the atmospheric chemistry experiment Fourier-transform spectrometer. Appl Opt 2005;44:7218–31.
[12] Lisak D, Rusciano G, Sasso A. An accurate comparison of lineshape models on H_2O lines in the spectral region around 3 μm. J Mol Spectrosc 2004;227:162–71.